Oxygen-controlled phase segregation in poly(N-isopropylacrylamide)/Laponite nanocomposite hydrogels

Henrik Mauroy[*,a], Zbigniew Rozynek[b], Tomás S. Plivelic[c], Jon Otto Fossum[b], Geir Helgesen[a], Kenneth D. Knudsen*[*,a]*

[a]Physics department, Institute for Energy Technology, P.O. Box 40, N-2027 Kjeller, Norway

[b]Department of Physics, Norwegian University of Science and Technology, Hoegskoleringen 5, N-7491 Trondheim, Norway

[c]MAX IV Laboratory, Lund University, P.O. Box 118, SE-221 00 Lund, Sweden

*E-mail: Henrik Mauroy: henrik.mauroy@ife.no; Kenneth D. Knudsen: kenneth.d.knudsen@ife.no

The combination of nanoparticles and polymers into nanocomposite gels has been shown to be a promising route to create soft materials with new or improved properties. In the present work we have made use of Laponite nanoparticles in combination with a poly(N-isopropylacrylamide) (PNIPAAM) polymer, and describe a phenomenon taking place during polymerization and gelling of this system. The presence of small amounts of oxygen in the process induce two distinctly separated phases, one polymer rich and one polymer deficient water-clay phase. Complex interactions between clay, oxygen and the polymer are found to govern the behavior of these phases. It is also observed that the initial clay concentration can be used to directly control the volume fraction of the polymer-deficient phase. The dynamics of the phase boundary is found to be dependent on water penetration, and in general to present

a non-Fickian behavior. An approach using video recording for monitoring hydrogel swelling is also presented and its advantages addressed.

Nanocomposite hydrogel, clay, Laponite, PNIPAAM, phase segregation, small angle x-ray scattering

1. Introduction

Nanocomposite hydrogels (NC-gel), a type of stimuli responsive soft materials, have received considerable attention over the last ten years.[1,2] These materials consist of clay nanoparticles embedded in a polymer matrix swollen with water. They were invented by Haraguchi et al.[1] who discovered that by adding only a few weight percent of the synthetic hectorite-clay, Laponite®, to an aqueous solution of N-isopropylacrylamide (NIPAAM) before carrying out the polymerization reaction, the usual syrup-like hydrogel that this particular polymer creates, did not emerge. Instead a solid rubber-like hydrogel, called a nanocomposite gel (NC-gel), was produced. In this gel the clay nanoparticles themselves acted as physical cross-links, homogenously dispersed in the polymer network. Mixing the pristine clay into a water-PNIPAAM solution did not result in a similar material. Furthermore, it was reported that the NC-gels could only be obtained by disc shaped inorganic particles such as clay.[3] However, recently a similar NC-gel utilizing alumino-silicate nanotubes have successfully been prepared.[4] This suggests that the formation of NC-gels is highly related to the dimensional properties of the filler particles and to physical interactions between the polymer and the surface of the particles.

The NC-gels exhibits remarkable properties such as extraordinary mechanical toughness and large reversible stretching abilities. They are also transparent, whereas chemically cross-linked gels are often opaque and also brittle, caused by their high and unevenly distributed cross-link density. Up to now extensive research has been carried out on the NC-gels for the mechanical and optical properties,[5-7] network structure [8-10] and different applications, such as dye absorption from industrial waste water,[11] self-healing polymeric materials,[12] thermally controlled micro-channel switches,[13] and biocompatible materials highly susceptible to magnetic fields.[14]

The formation of NC-gels is a complex process which involves several reactions and interactions between its constituents (water, monomer, accelerator, initiator, clay, cations and polymer chains). This was thoroughly deduced and explained in detail by Haraguchi et al.[3] The main steps are as follows: Prior to polymerization, inside the reaction solution, NIPAAM interacts strongly with the surface of the dispersed Laponite platelets. Hydrogen bonding between the amide group of NIPAAM and the terminating oxide and hydroxyl groups of the clay surface provides attraction between the monomers and the clay platelets, resulting in coverage of the clay platelets by NIPAAM monomer. This prevents the Laponite from forming "the house-of-cards" network structure[15,16] by shielding the attractive potential between negative platelet surfaces and positive platelet edges on neighbor platelets,[3] even though the salt concentration in the solution is high due to the presence of a significant amount of the polymerization initiator potassium peroxodisulphate (KPS). After initiation of the polymerization reaction, a large number of polymer chains are believed to start growing outwards from each platelet, forming "clay-brush particles",[3,17] and eventually a continuous network of polymer chains cross-linked by clay platelets is formed (Figure S1).

In this work on PNIPAAM-Laponite NC-gels we have studied in detail how it is possible to induce phase segregation and control the phase composition by adding small quantities of oxygen prior to polymerization. PNIPAAM is most easily prepared using the radical polymerization technique, and it is normally important to avoid any oxygen in the reaction solution, since O_2 will act as a competing radical and hinder the polymerization. However, by adding controlled amounts of oxygen the system segregates during polymerization into two transparent phases with different composition, separated by a sharp transition (phase boundary), where the volume of the top phase is directly related to the initial Laponite concentration. These effects are illustrated in Figure 1, which we will comment more on later. Here the phase boundary (marked with arrows) in each sample can be seen as a white or dark ring below the meniscus.

The present paper investigates in detail the above-mentioned behavior, with particular emphasis on how controlled amounts of oxygen influences the formation of the two-phase system, as well as the

dynamics of the boundary between the two phases. In order to probe the composition of the phases and the displacement of the interfacial region, we use a combination of small angle x-ray scattering (SAXS), thermal gravimetrical analysis (TGA), and image analysis. Furthermore, we suggest how these observations can be relevant in new studies of nanoparticle-polymer systems.

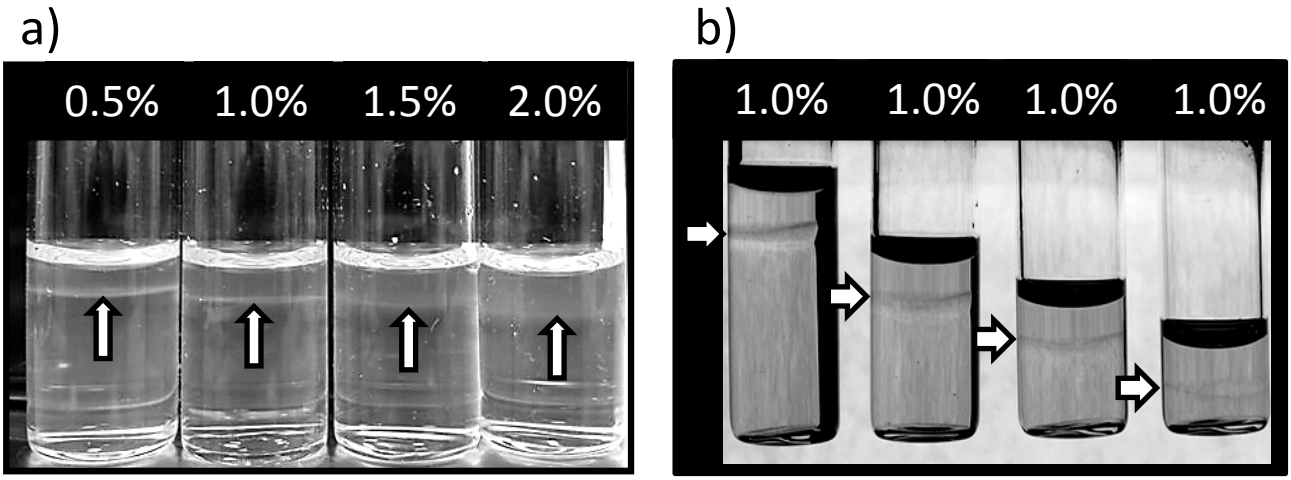

Figure 1. a) Four PNIPAAM-Laponite samples with different clay concentrations, from left 0.5, 1.0, 1.5 and 2.0 wt.%. b) Backlit picture of four different volumes of the exact same reaction solution (1 wt.% Laponite and 10 wt.% NIPAAM), with the volumes from left: 3.0, 2.0, 1.5, and 1.0 mL. The position of the phase boundary in both pictures is marked by arrows.

2. Experimental section

2.1. Materials

N-isopropylacrylamide (NIPAAM, ≥98 %) was purchased from Polysciences Inc., Laponite XLG (≥99 %) was kindly supplied by Andreas Jennow AB, Tetramethylethylenediamine (TEMED, ≥99 %) and potassium peroxodisulphate (KPS, ≥ 99 %) were purchased from Sigma-Aldrich. All chemicals were used as received, and all solutions used in the experiments were prepared in deionized water.

2.1.1. Laponite XLG

Laponite is a synthetic layered silicate with the approximate chemical formula $Na_{0.7}[Mg_{5.5}Li_{0.3}Si_8O_{20}(OH)_4]$. At low concentrations in water (1-5 wt.%) it exfoliates almost completely into single platelets with a diameter of about 30 nm and a thickness of 1 nm.[18] The platelets carry a

negative charge, due to isomorphous substitution of Mg^{2+} by Li^{+} ions, resulting in a unit cell charge of -0.7e. These elementary charges (roughly -700e in total) are uniformly distributed over the discs, and are counterbalanced by Na^{+}-ions located between the platelets in the crystalline form. A smaller positive charge, counterbalanced by adsorbed hydroxyl groups where the crystal structure terminates, is concentrated along the rim of the disc.

2.2. Preparation of NC-gels

The general method of producing NC-gels using the free-radical polymerization technique can be found in the literature.[1,19,20] In our work the NC-gels were prepared using initial solutions consisting of monomer (NIPAAM), cross-linker (Laponite XLG clay), accelerator (TEMED), and initiator (KPS). In all samples, the water/monomer ratio, monomer/initiator ratio and the volume of the accelerator were fixed at 10/1 (w/w), 100/1 (w/w) and 10 μL/g NIPAAM, respectively.

First 200 mL of deionized water was stirred with a magnetic stirrer inside a glove bag filled with a controlled amount of nitrogen- and oxygen-gas. The partial pressure of oxygen (pO_2) was monitored with a Lutron DO-5510 oxygen meter capable of measuring both O_2% and dissolved oxygen (DO). The water was stirred until the DO-level was stable (approx. 1 h). The DO-level (mg/L) was found to follow the relationship $DO = 0.30(\pm0.02)\cdot pO_2 + 0.95(\pm0.2)$, calculated by linear regression of the data points in Figure S2.

Still inside the glove bag, 2.0 g of Laponite XLG was then added to 100 mL of the oxygen-saturated water and stirred for 30 minutes. The Laponite-dispersion was divided into several glass vials, and the desired amount of oxygen-saturated water was added to each vial in order to arrive at the desired Laponite concentration. Subsequently 0.1 g NIPAAM was added to each sample vial and solubilized by hand shaking until a clear and homogenous solution was achieved. 1.0 μL TEMED was then added to each vial which were shaken for 30 seconds and left to rest in an ice bath for 30 minutes. Finally, 80 μL of KPS-solution (25 mg/mL) was added to each sample, which was hand shaken for 10 seconds and immediately put back into the ice bath (0 °C). After approximately 5 minutes all the samples were taken out of the glove bag and removed from the ice bath in order to start the polymerization reaction, and

subsequently placed in a custom camera-rig at room temperature. The samples were mounted on an aluminium stage in front of a fluorescent light panel which kept the surrounding temperature at approximately 27.5 °C. The temperature of the solutions was checked with an infrared thermometer.

In this paper we express the Laponite concentration in each sample as a percentage of the water-content. For instance, a 1 wt.% concentration equals 0.01 g Laponite dissolved in 1 g of water, and the resulting NC-gel is labeled NC1.

2.3. Characterization

2.3.1. Monitoring of the polymerization reaction

A Nikon EOS 550D SLR-camera with a resolution of 2592x1728 pixels was used to record images each minute during polymerization. A light panel was used to backlit the samples during imaging, which lasted over a period of up to 12 hours. The images were converted to high-speed movies for further analysis with the software package Matlab from MathWorks®. The movies were examined visually to monitor changes in transparency in the samples, and to follow both the formation and displacement of the phase boundary. In the analysis the displacement was tracked by measuring the number of pixels that the phase boundary moved from one frame to another. The translation of the phase boundary was quantified by relating the displacement to the initial height of the bottom phase. Fitting procedures and data manipulation were performed with the software package Origin®.

2.3.2. Small angle x-ray scattering (SAXS)

The SAXS experiments were performed at beamline I911-4 of the MAX-lab synchrotron facility in Lund, Sweden.[21] All data were collected at a wavelength of 0.91 Å with a sample-to-detector distance of 1.9 m, resulting in a covered q-range of about 0.01-0.3 $Å^{-1}$ (q is the magnitude of the scattering vector and is defined as $q=(4\pi/\lambda)\ sin(\theta)$ with λ being the wavelength and 2θ the scattering angle). The beam size at the sample position was approximately 300 x 300 microns. The detector used was a two-dimensional CCD (165 mm diameter from Mar Research, Inc). The reaction solutions were kept in standard 2 mm round sealed borosilicate glass capillaries. For the *in situ* polymerization study, the samples were continuously scanned at different points along the central axis of the capillaries, with an

exposure time of 15 seconds at each point. The whole scan was repeated at the same points, with up to 10 repetitions. The duration of each scan was approximately 9 minutes, which thus defines the time resolution at each point. Data treatment was performed using the software FIT2D [22] and customized Matlab® routines. The data were normalized by the transmitted intensity with a photodiode located inside the beam-stop and corrected by the background and water scattering contribution.

2.3.3. Thermal gravimetrical analysis (TGA)

TGA was performed on a Netsch STA 449 F3 Jupiter TGA-DSC instrument from 25 to 650 °C under Argon atmosphere with a heating rate of 10 °C/min. Other instrumental parameters were adjusted with the software package STA 449F3. A 70 μL alumina crucible was used to hold the samples which weighed between 10 and 25 mg.

3. Results and discussion

3.1. Polymerization dynamics

The image monitoring of the NC-gels during polymerization showed that the phase segregation takes place in several stages. This behavior is illustrated in Figure S3 for an NC0.5-gel polymerized in 10 % O_2-atmosphere. The times given in the figure are only representative for this sample because both clay concentration and oxygen partial pressure determine the starting time for each stage, as discussed later in section 3.6. The first stage (not shown in the figure) is characterized by a small but gradual decrease in transparency for the whole sample volume, during which the polymer-clay brushes grow and start to scatter light. A simultaneous small increase in temperature, up to 28-30 °C, was observed due to energy being released from the polymerization reaction.

The first stage is followed by a relatively rapid stage, of 5-15 min duration, characterized by a sudden and complete loss of transparency in the lower volume of the sample (Figure S3b). This occurs due to the significant hydrophobic interactions which normally takes place above the lower critical solution temperature (LCST) of PNIPAAM, at approximately 32 °C.[23,24] Above this temperature long PNIPAAM chains associate into denser hydrophobic entities with a size comparable to optical wavelengths, leading to internal light scattering in the solution. Examination of the samples at this stage revealed that the

opaque region consisted of a continuous NC-gel with inferior mechanical properties compared to fully polymerized NC-gels. This indicates that the polymer chains were too short to produce a well cross-linked network with the clay particles. The time scale of this opaque state was almost unaffected by the Laponite concentration, but increased with pO_2 (Figure S4).

Subsequently a third state occurs, characterized by a relatively brief (6-15 min duration) recovery of transparency for the lower sample volume (Figure S3c). Our interpretation is that the polymer chains have now grown sufficiently long to create strong inter- and intrachain hydrophobic associations, and thus these PNIPAAM clusters will expel water and shrink enough to reduce scattering in the visible range.[25] The end of this state is characterized by the establishment of a visible phase boundary (Figure S3c), separating a polymer-deficient top phase and a polymer-rich bottom phase, that will be discussed later. The phase boundary is visible due to the difference in refractive index between the two phases. At this point the polymerization reaction is nearly completed because the bottom phase behaves like a typical NC-gel prepared in the absence of oxygen (rubber like and highly flexible). This was confirmed by analyzing the phase in a situation where the polymerization reaction had been stopped by rapid cooling right after the appearance of the phase boundary.

In the fourth and last stage, which lasts for several hours, depending on the oxygen concentration, the phase boundary is found to move upwards in the reaction vessel (Figure S3d). This displacement was discovered to be caused by water being absorbed from the top phase into the polymer-rich bottom phase, thereby increasing the volume of the latter. This effect will be discussed later in section 3.2 and 3.5. The decrease of water in the top phase effectively increases the clay and initiator (KPS) concentration in this phase, leading to the formation of a clay-water gel with a drastically higher viscosity, caused by the clay network structure now being formed.

The final volume of the top phase for these systems was found to be directly determined by the initial Laponite concentration. Increasing the concentration of clay lead to a top phase with a correspondingly larger volume, as seen in Figure 1a where four NC-gels with Laponite concentrations of 0.5, 1.0, 1.5 and 2.0 wt.% are shown. Further evidence for this behavior is given in Figure 1b where we show four NC1-

gels prepared from one reaction solution, but with different total volumes. Notice that the volumes of the top phases of these samples are now almost identical, independent of the total volume. Varying the partial pressure of oxygen also affected the volume of the top phase. It was found to be linearly dependent on the oxygen pressure, as shown by the regression lines in Figure 2, which shows the relative volume of the top phase as a function of pO_2. We believe this effect to be due to a direct relationship between dissolved oxygen in the solution and the resulting termination of growing polymer chains, i.e. more oxygen decreases the number of chains and thus their effective total volume. Further discussions will be given later in section 3.7.

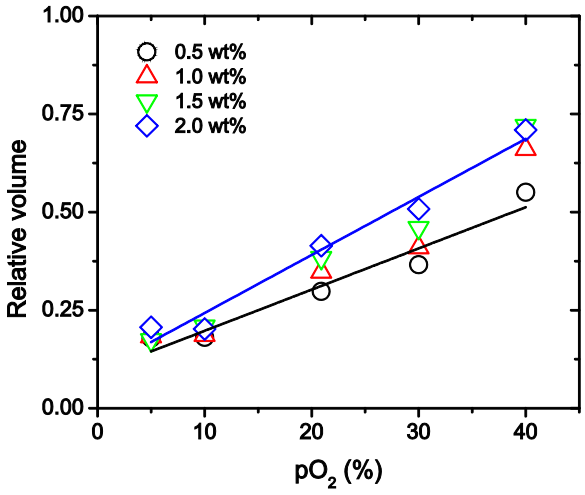

Figure 2. Relative volume of the top phase vs. pO_2. The data points for the 0.5 wt.% and 2.0 wt.% samples are fitted with regression lines.

3.2. Small angle x-ray scattering (SAXS)

The X-ray scattering from NC-gels, or NIPAAM-clay solutions, will be dominated by the signal from the clay particles, due to the much larger electron density contrast of the clay to the water solution compared to that of the NIPAAM units.[10,26] This is contrary to small angle neutron scattering where the polymer contribution can be seen based on the differences in scattering length density between the polymer and the solvent.

SAXS-curves from a series of NIPAAM-Laponite solutions (with clay contents ≤ 2 wt.%) are shown in Figure S5. As expected from dilute dispersions of randomly oriented thin discs, the scattering

intensity in the mid *q*-range follows a power law, i.e. $I(q) \propto q^{-\alpha}$, where $\alpha = 2$.[27] The scattering curve from a 1.0 wt.% Laponite-H_2O solution without monomer, also presented in Figure S5, is practically overlapping with that of the 1.0 wt.% solution with monomer, demonstrating the negligible contribution from the monomer to the overall SAXS signal. Three of the curves, 1.0, 1.5 and 2.0 wt.%, were fitted using the form factor for thin discs [28] (eq. 1) where, *R* and *2H* are the radius and thickness of the particles, respectively, $J_1(x)$ is the first order Bessel function, α is the angle between the axis of the disc and the scattering vector *q*, $(\rho_{e,clay}-\rho_{e,H2O})$ is the electron density contrast between the Laponite platelets and water, N_{clay} is the number of clay platelets per unit volume, and v_{clay} is the volume of a single disc. For comparison, also the Guinier approximation for thin discs (eq. 2), was employed to determine the particle thickness. The fits are displayed in Figure 3 and the detailed results can be found in Table T1.

$$I(q) = \left(\rho_{e,clay} - \rho_{e,H2O}\right)^2 N_{clay} v_{clay}^2 \int_0^{\pi/2} \left[\frac{2J_1(qR\sin\alpha)}{qR\sin\alpha} \frac{\sin(qH\cos\alpha)}{qH\cos\alpha} \right]^2 \sin(\alpha) d\alpha \qquad (1)$$

$$I(q)q^2 \propto \exp\left[-\frac{(2H)^2 q^2}{12} \right] \qquad (2)$$

The two methods gave similar values for the thickness, of approximately 1.6 nm, and the thin disc model resulted in a diameter of around 42 nm. These results are not far from nominal values for fully exfoliated Laponite platelets, approximately 1 and 30 nm, respectively. However, the slight increase found with respect to the nominal thickness of 1 nm indicates that a small amount of not fully exfoliated particles may be present, thus increasing the average value.

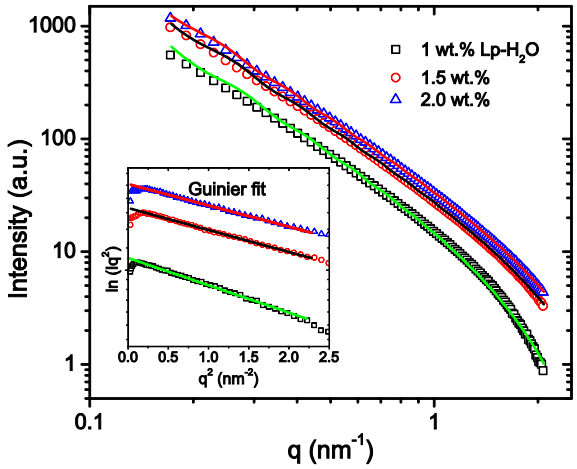

Figure 3. Fittings of the scattering curves using eq. 1 for: 1 wt.% Laponite with no monomer (black squares), 1.5 wt.% Laponite (red circles) and 2.0 wt.% Laponite (blue triangles), respectively. The fit is shown with continuous lines. The inset shows Guinier fits for the same SAXS-curves. Every 10th data point is shown for clarity.

A clear linear relationship between scattering intensity and Laponite concentration is also observed in the data in Figure S5, as expected from eq. 1. The scattered intensity will depend on the differences $(\rho_{e,clay} - \rho_{e,H2O})^2$ and $(\rho_{e,PNIPAAM} - \rho_{e,H2O})^2$ plus a cross-term $(\rho_{e,clay} - \rho_{e,H2O})(\rho_{e,PNIPAAM} - \rho_{e,H2O})$, where $\rho_{e,clay} = 7.98 \times 10^{23}$ *electrons/cm*^{3}, $\rho_{e,PNIPAAM} = 4.16 \times 10^{23}$ *electrons/cm*^{3}, *and* $\rho_{e,H2O} = 3.34 \times 10^{23}$ *electrons/cm*^{3}. Thus the terms due to PNIPAAM are in this respect much smaller than that of the clay, and can here be neglected. It is therefore possible to qualitatively follow the changes with time of the clay concentration, in the top- and bottom-phase, by time resolved SAXS, assuming that clay-clay interactions during the polymerization process are not significantly contributing to the scattering signal.

Several samples were therefore continuously scanned, along a line that later crossed the phase boundary (inset Figure 4a), while collecting SAXS images during the course of polymerization. As an example Figure 4a displays the scattering curves of an NC1.5-gel polymerized in 5 % O_2 atmosphere from a point 1 mm above and a point 1 mm below the phase boundary at two different times of the reaction. Figure 4b shows the time-evolution of the Laponite concentration in these two small volumes. The concentration was calculated by normalizing the *in situ* SAXS-curves to the curve of the 2.0 wt.%

Laponite-monomer solution in Figure S5, over the *q*-range 0.17-1 nm^{-1}. After 10 minutes of polymerization the concentration is almost equal in the two volumes, above and below the phase boundary respectively, showing that the clay is evenly distributed in the sample. After this, the concentration in the lower volume decreases gradually, and at 90 minutes, it has decreased by around 60 % compared to the initial value. The upper volume, on the other hand, experiences a small concentration increase in the same time frame.

The reason for these changes is that water is extracted from the upper volume and absorbed by the polymer chains which at this time are located below the phase boundary (cfr. section 3.1). As the water crosses the phase boundary it will significantly dilute the small volume which is probed in Figure 4. Since the clay particles in the upper volume are too large to diffuse into the polymer phase below, they will remain in the upper volume and the concentration here will be raised.

Results from fitting the SAXS-data at the two different times, can be found in Table T2. Both fitting procedures show that the thickness of the Laponite particles in the bottom phase increases slightly, to around 2 nm during polymerization. The reason for this may be the reduced screening as the monomer is consumed, which results in an easier stacking of the clay platelets when the monomer no longer covers the particles.

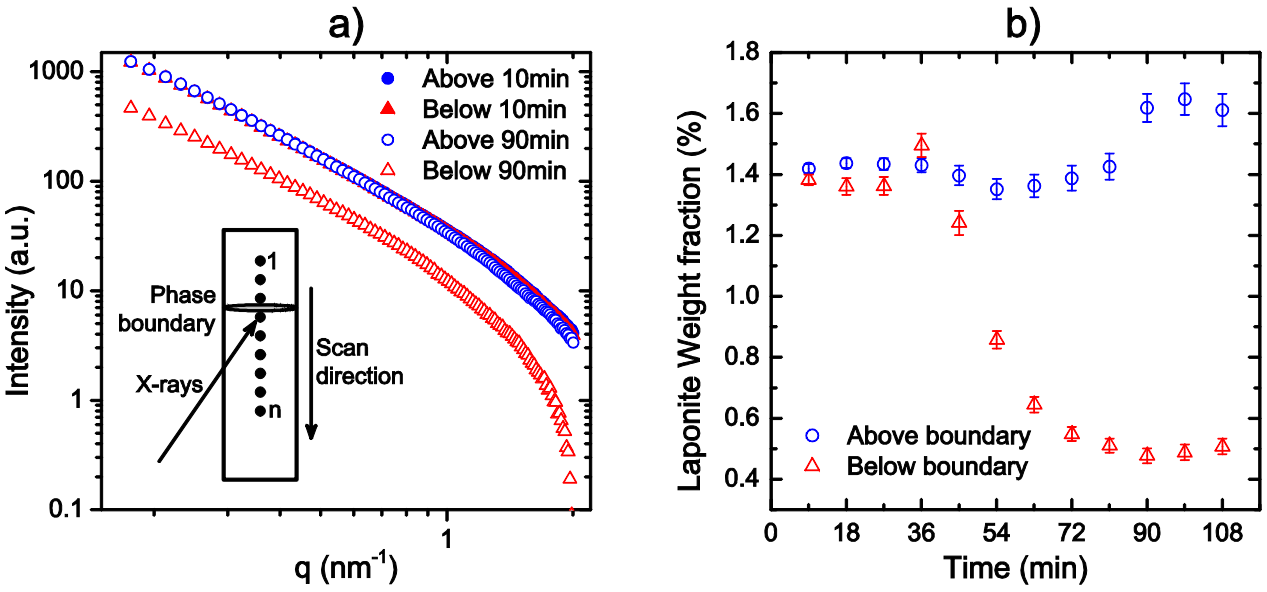

Figure 4. a) *In situ* SAXS curves of an NC1.5-gel at two different times for a point 1 mm above (blue symbols) and 1 mm below (red symbols) the phase boundary. Inset is a sketch of the *in situ* SAXS setup. b) The time-evolution of the Laponite concentration in the two phases above and below the phase boundary, respectively. The error bars are the standard deviations.

These results thus show that the concentration of Laponite near the phase boundary changes during polymerization. It's important to mention that the large concentration decrease observed in the lower volume only extends a short distance downwards in the samples because the relative increase in water content is highest close to the boundary. The final concentration in each volume however, occurs after 12-24 hours, and could not be quantified directly by these *in situ* SAXS experiments due to the limited time available at the synchrotron.

3.3. Thermal gravimetric analysis

In order to probe the differences in polymer content in each of the two phases, thermal gravimetrical analysis (TGA) was performed on several NC-gels, with different clay concentrations. The top and bottom phases were measured separately. Figure 5a shows TGA-curves from pure NIPAAM, and from one of the NC-gels, representing the typical behavior that was found for these samples. Both curves from the NC-gel show a prominent mass loss around 100°C, attributed to loss of water. The corresponding differentiated curves (DTGA) are shown in Figure 5b. The peak around 150-175 °C corresponds to evaporation of the monomer. The top phase loses its remaining mass in this step, indicating that it contained a significant amount of monomer. The bottom phase, on the other hand, does not display a sharp peak in this step, showing that only small amounts of monomer were present. The third peak around 350-400 °C corresponds to decomposition of the polymer chains. Besides water evaporation, most of the mass in the bottom phase is lost in this step. The top phase also shows a small decrease in the same region, indicating the presence of a small quantity of polymer chains, but less than 0.5 wt.%.

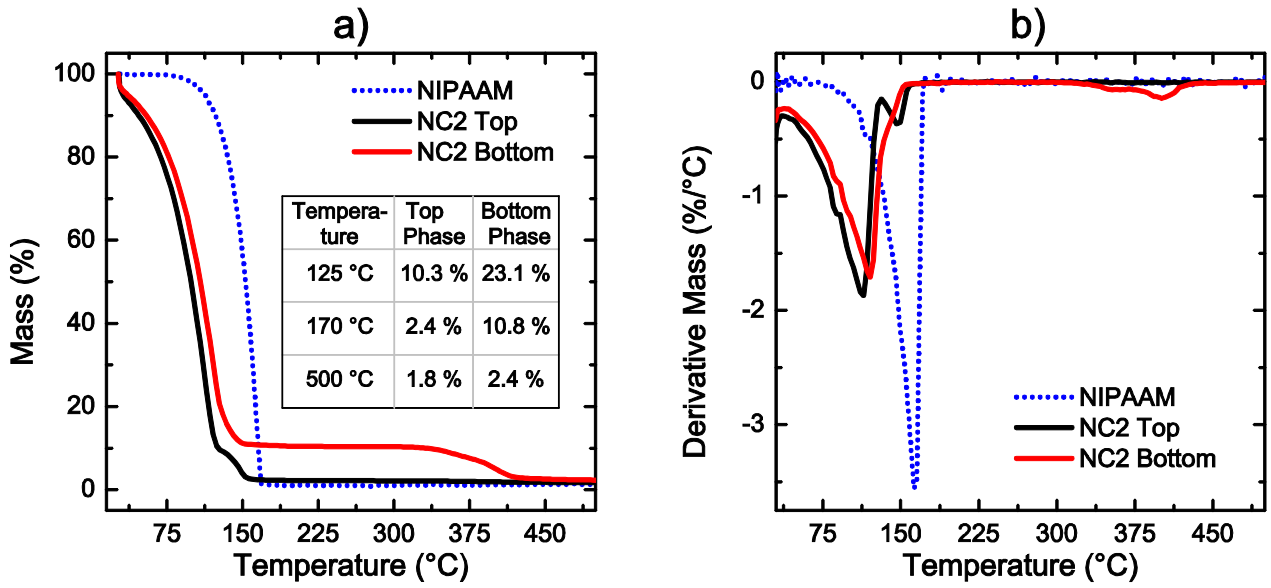

Figure 5. a) TGA-curves of the top- and bottom-phases of an NC2-gel (solid black and dashed red, respectively). Pure NIPAAM monomer (dotted blue) is shown for comparison. The inset shows the remaining mass in each phase at 125, 170 and 500 °C, respectively. b) DTGA curves of the same samples.

The remaining mass% at three temperatures are presented in the inset in Figure 5a. At 125 °C, the mass left in the top phase is just above the starting monomer concentration (10 %), indicating that all water has been released. The bottom phase still contains around 13 mass% water, caused by water bound to the polymer chains. At 170 °C all water and monomer have been released from the top and bottom phases, which now contains 2.4 and 10.8 mass%, respectively. At 500 °C the remaining mass (~2 %) in the two phases is a mix of clay and char from the polymer. It was expected, based on the SAXS-results, that the remaining weight fraction would be highest in the top phase. The reason for a slightly lower value here may a smaller amount of char in the top phase, since the monomer evaporates at elevated temperatures rather than turning into char. It is also important to note that the large decrease in concentration of 60 % in the bottom phase, calculated from SAXS-curves, takes place only close to the phase boundary and not throughout the entire volume.

3.4. Physical characteristics

As a consequence of the strong hydrophobic interactions above LCST, water solutions of PNIPAAM or PNIPAAM NC-gels become turbid. If the polymer concentration is above a few weight percent, the solutions/hydrogels become completely opaque and white. Heating the two-phase NC-gels above the LCST of 32 °C revealed that the top phase did not contain polymer chains with sufficient length to undergo this transition, confirming our conclusions from the TGA-experiments. For the bottom phase the transition manifests itself as a drastic loss in transparency and contraction of the polymer hydrogel (see Figure 6A). This transition was found to be reversible for all samples.

It is well known that Laponite-water dispersions create shear-thinning gels by forming a network structure often referred to as the "house-of-cards" structure[15,16] if the salt concentration is high enough, and it was found that the top phase of these samples behaved like such a physical gel (see Figure 6B). At concentrations below one weight percent the top phase flowed almost freely, whereas samples with higher clay particle concentrations had to be subjected to a hard impact before the top phase would flow. The cause of the gel-formation is the increase in salt concentration due to the KPS-initiator while the bottom phase is absorbing water. The bottom phase on the other hand, exhibited similar physical properties as an NC-gel prepared in absence of oxygen. The phase boundary is marked by arrows in the figure. These observations corroborate the results from SAXS and TGA concerning the composition of the two phases.

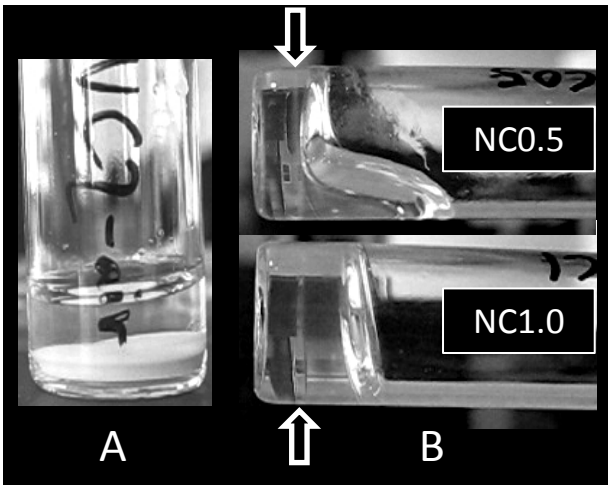

Figure 6. A) An NC2-gel displaying the more dense high-temperature conformation (> 32 °C) of the polymer phase, seen as a white disc at the bottom. B) The top phase in an NC0.5-gel exhibits shear thinning behavior after being tilted, while an NC1-gel is rigid.

3.5. Swelling kinetics

Once the phase boundary has appeared in the samples, it starts to translate upwards and becomes more diffuse with time due to water being absorbed into the bottom phase. The relative movement of the boundary was extracted via image processing of a large series of images taken during polymerization. If these data are plotted double logarithmically as suggested by Lee et al.,[29] when they measured swelling kinetics of PNIPAAM-Montmorillonite gels, the slope of the regression line through the data points would give the exponent n in the heuristic equation (3)

$$\frac{W_t}{W_\infty} = Kt^n \qquad (3)$$

where W_t and W_∞ are the weight of the gel at a time t and at infinite time (end of the process), respectively, and K is a characteristic constant of the gel. Based on equation 3, the movement s of the boundary will also be given by $s=Kt^n$. If $n \leq 0.5$, penetration of water molecules into the gel will follow the normal Fickian behavior, and if $0.5<n<1$, the process corresponds to non-Fickian anomalous diffusion.[20,30] Crank[30] interpreted the distinction based on the speed of which the material responds to changes in its conditions. In Fickian processes, the rate of diffusion is thus much less than that of relaxation, while a non-Fickian behavior is described by a much faster diffusion than relaxation. Deviations from Fickian normal diffusion are considered to be associated with the finite rates at which the polymer structure may change in response to the sorption or desorption of penetrant molecules.

A double logarithmic plot of our data showed that the slope of the curves was not affected by the oxygen concentration, but varied with the Laponite concentration. As an example, the relative movement of the phase boundary in NC0.5-gels (0.5 wt.% Laponite) polymerized with varying oxygen atmosphere (pO_2) is presented in Figure 7. The kinetic exponent n was calculated for NC-gels with four different Laponite concentrations, by fitting similar data as in Figure 7 with $s=Kt^n$, and the average n-

values are shown in the inset. For all samples these values indicated non-Fickian diffusion, i.e. $n > 0.5$, but there was also a gradual increase with increasing clay concentration. This behavior is most likely due to the correspondingly lower relaxation rate (stiffer gel) as the concentration increases, since the number of cross-linking points is directly controlled by the amount of Laponite present.

Zhang et al.[20] performed a swelling study on PNIPAAM-clay gels with different clay types, and obtained an *n*-value of 0.44 for a similar NC-gel containing 2.0 wt.% Laponite. Our higher values may be attributed to differences in how the measurements were performed. The main factors which have to be taken into account here is that swelling studies are usually performed by drying the gel completely, and then immersing it into deionized water. In the present study the gels were not dried from the start, and the water they could absorb contained ions and unreacted monomer molecules. However, the prospect of monitoring swelling by video recording is interesting, as it opens up the possibility of measuring the gel dynamics continuously, and over extended periods of time, without interference.

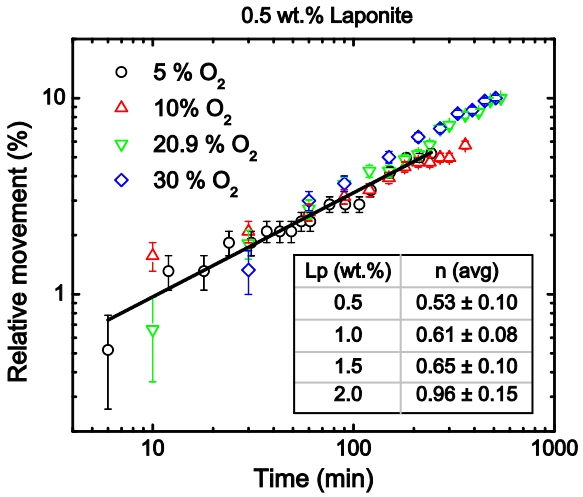

Figure 7. Relative movement of the phase boundary in NC0.5-gels versus time after appearance of the phase separation, for four different experiments with varying pO_2. The error bars correspond to a translation of one pixel in the images. The solid line is a regression fit to the 5 % O_2 data points. The inset shows the average kinetic exponent *n* calculated for NC-gels with different Laponite concentrations prepared in varying pO_2.

3.6. Polymerization kinetics

The time delay before the samples became opaque (second stage, Figure S3b) was found to be almost linearly dependent on the clay concentration. This relationship is shown in Figure 8a, where time is plotted versus initial clay concentration. This behavior can be explained by the lower mobility for monomers as the concentration of obstructing clay platelets is increased in the solution. The lowered mobility delays the growth of polymer chains, and hence the time for the chains to aggregate into clusters that scatter light. A similar tendency was found with respect to increasing pO_2, as seen in Figure 8a, and plotted separately in Figure 8b. Here, the linear increase in time is a result of the suppression of polymer growth by the dissolved oxygen as the oxygen pressure is raised.

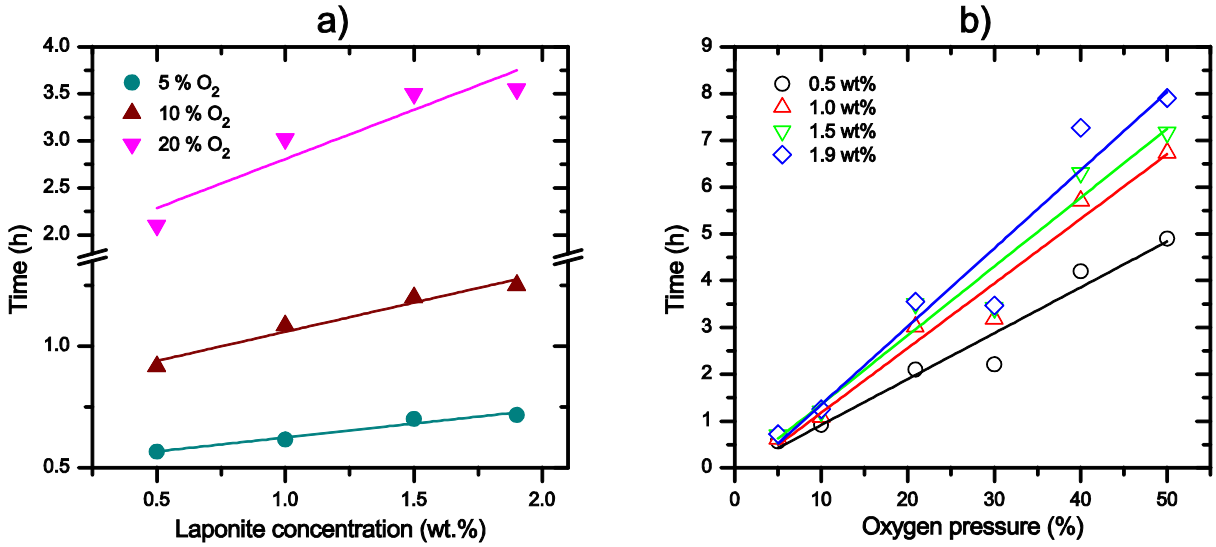

Figure 8. Time for the NC-gels to become opaque, as a function of a) clay concentration and b) the partial pressure of oxygen (pO_2). The solid lines are regression fits to the data.

3.7. Mechanism behind the phase segregation

After considering in detail the various effects described in section 3.1-3.6, we believe that a plausible mechanism for the phase separation during polymerization and the dynamics of the phase boundary is as follows. At an early stage, when clay-brush particles are being formed, the dissolved oxygen can react with the growing polymer chains, thereby terminating these. As a result two populations of particles can be formed, namely oxygen-terminated (OT) and non-terminated (NT) particles. Specifically, the latter

describe either partially oxygen-terminated or not terminated at all. Considering the amphiphilic nature of PNIPAAM, both populations of clay-brush particles will be amphiphilic, but an OT-particle will have a relatively more hydrophilic nature due to the more polar oxygen-terminated chain ends. The hydrophobic component of the clay brush particles is likely to be due to an outer layer of N-isopropyl groups, as commented by Haraguchi et al.[31] The OT-particles will now tend to avoid the more hydrophobic constituents in the reaction solution, i.e. NT-particles, leading to a local phase separation at an early stage. Samples without clay exhibited the same segregation effects when polymerized in a partial oxygen atmosphere which demonstrates this prinsiple. Moreover, since PNIPAAM is slightly denser than water (1.17 g/cm^3 at 25°C) the water phase will be displaced upwards. Although the clay particles have twice the density of the polymer (2.5 g/cm^3), they are suspended due to their small size (~30 nm) and low concentration.

Later, during polymerization, the transparency of the bottom phase drops drastically when the chains have grown to a sufficient length to create strong hydrophobic associations. This effect is not observed for the top phase, since the OT-particles here are unable to polymerize further. The duration of the opaque phase was highly affected by the O_2 pressure, as shown in Figure S3, with more O_2 giving longer durations. This is most likely because the overall growth speed of the polymer becomes lower when the amount of dissolved oxygen is increased.

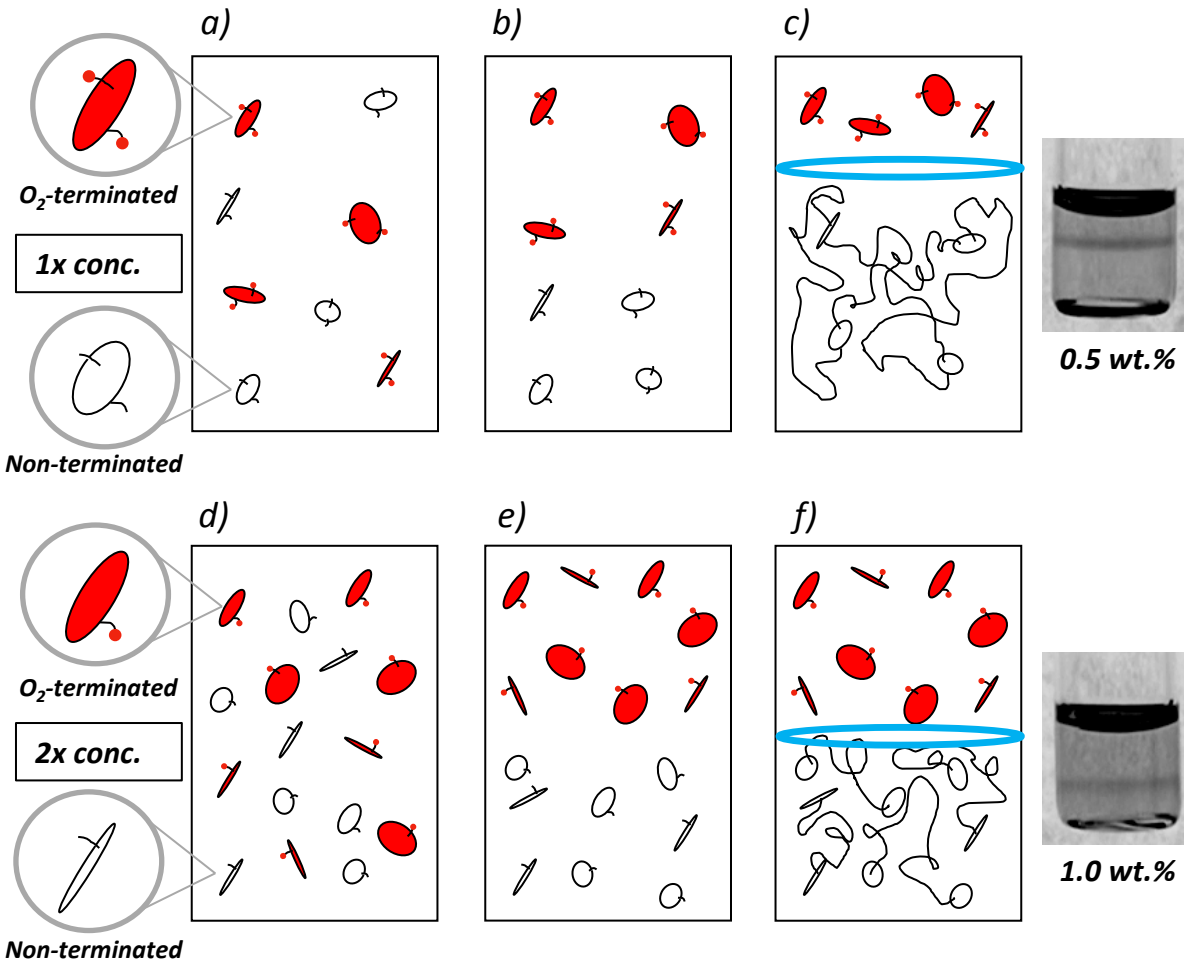

Figure 9. A schematic representation of the phase segregation taking place during polymerization of one low-concentrated sample (a-c) and one sample with twice the clay content (d-f). Non-terminated clay platelets are represented as white discs while the O_2-terminated platelets are represented as red discs, the polymers are represented as black lines, and the red dots are oxygen molecules terminating short polymer chains. The phase boundary is shown in blue. Right side: Pictures of the final stage for samples with two different concentrations.

The highly predictable volume ratios resulting from the phase segregation can be explained in detail by considering a mechanism where both diffusion and solubility of clay in water are relevant. A simplified scheme of the proposed mechanism of the phase segregation is shown in Figure 9. In samples of low clay concentration (Figure 9a), the number of polymer chains growing out from each clay particle will be higher as there will be more initiating persulphate radical per clay particle. E.g. in the scheme in

Figure 9, the particles in the upper sample have twice as many grafted chains as in the lower. In effect, more oxygen can react with each particle, and is thus distributed on fewer particles compared to the situation in a higher concentrated sample.

After the initial segregation of OT and NT clay-brush particles the volume fraction of the top phase in both samples are equal, assuming that the average particle density is maintained throughout the whole sample volume (Figure 9b and e). Now, while the polymerization proceeds in the bottom phase, the OT-particles will be forced further into the top phase by the hydrophobic entities in the bottom phase, thereby confining them to a smaller volume of water. This occurs until a critical concentration is reached in the top phase, when the “house-of-cards” network structure establishes.

A low-concentrated sample will at this point be able to reduce its volume in the top phase more than a higher concentrated sample, and as a result, the volume fraction ends up smaller (Figure 9c). On the other hand, OT-particles in a sample of high concentration will meet the conditions for a developed “house-of-cards” network structure earlier, and will thus experience a smaller volume decrease (Figure 9f). This is also demonstrated in the pictures of two such samples on the right side of Figure 9.

4. Conclusion

We report here the detailed description of a phenomenon taking place during polymerization of PNIPAAM-Laponite NC-gels. It is shown how small amounts of oxygen present in the reaction solutions induces phase segregation, resulting in a polymer rich phase distinctly separated from a polymer deficient water-clay phase. Reactions between oxygen and the growing polymer chains are the reasons for this effect, which produces two species of clay-polymer particles, where one has most of its chains oxygen-terminated at an early stage during the polymerization reaction. The resulting higher hydrophilic nature of these particles induces the phase separation. It was also revealed that in this system the initial clay concentration directly determines the final volume of the polymer deficient phase. We furthermore probed the dynamics of the phase boundary and showed how this is a non-Fickian process, and also a linear function of the clay concentration.

The phenomenon described here can be of value with respect to new ways of isolating surface treated nanoparticles, e.g. clay nanoparticles grafted with short oxygen-terminated polymer chains. A non-invasive technique, using video recording for monitoring swelling studies of hydrogels, was also extensively used. This application, scarcely observed in the literature, brings the possibility of measuring the gel dynamics continuously and over extended periods of time, without interference.

5. Acknowledgements

The authors gratefully acknowledge the financial support provided by The Research Council of Norway, and MAX-Lab for the X-ray beam time provided.

Supporting Information Available: Figure S1: A schematic representation of the NC-gel network structure. Figure S2: Relationship between the amounts of dissolved oxygen in deionized water as a function of the partial oxygen pressure. Figure S3: Snapshots of the different stages during the polymerization reaction. Figure S4: Duration of the opaque state during polymerization as a function of the partial oxygen pressure. Figure S5: SAXS curves of water-NIPAAM-clay solutions. Table T1 and Table T2: SAXS fitting results. This information is available free of charge via the Internet at http://pubs.acs.org/

6. References

(1)Haraguchi, K.; Takehisa, T. Nanocomposite hydrogels: A unique organic-inorganic network structure with extraordinary mechanical, optical, and swelling/de-swelling properties. *Adv. Mater.* **2002**, 14, 1120-1124.

(2)Haraguchi, K.; Murata, K.; Takehisa, T. Stimuli-Responsive Nanocomposite Gels and Soft Nanocomposites Consisting of Inorganic Clays and Copolymers with Different Chemical Affinities. *Macromolecules* **2012**, 45, 385-391.

(3)Haraguchi, K.; Li, H. J.; Matsuda, K.; Takehisa, T.; Elliott, E. Mechanism of forming organic/inorganic network structures during in-situ free-radical polymerization in PNIPA-clay nanocomposite hydrogels. *Macromolecules* **2005**, 38, 3482-3490.

(4)Liu, M.; Li, W.; Rong, J.; Zhou, C. Novel polymer nanocomposite hydrogel with natural clay nanotubes. *Colloid. Polym. Sci.* **2012**, 290, 895-905.

(5)Haraguchi, K. Stimuli-responsive nanocomposite gels. *Colloid. Polym. Sci.* **2011**, 289, 455-473.

(6)Wang, T.; Liu, D.; Lian, C.; Zheng, S.; Liu, X.; Tong, Z. Large deformation behavior and effective network chain density of swollen poly(N-isopropylacrylamide)-Laponite nanocomposite hydrogels. *Soft Matter* **2012**, 8, 774-783.

(7)Ren, H.-y.; Zhu, M.; Haraguchi, K. Characteristic Swelling-Deswelling of Polymer/Clay Nanocomposite Gels. *Macromolecules* **2011**, 44, 8516-8526.

(8)Shibayama, M.; Karino, T.; Miyazaki, S.; Okabe, S.; Takehisa, T.; Haraguchi, K. Small-angle neutron scattering study on uniaxially stretched poly(N-isopropylacrylamide)-clay nanocomposite gels. *Macromolecules* **2005**, 38, 10772-10781.

(9)Osaka, N.; Endo, H.; Nishida, T.; Suzuki, T.; Li, H.-j.; Haraguchi, K.; Shibayama, M. Microphase separation in nanocomposite gels. *Phys. Rev. E* **2009**, 79.

(10) Nishida, T.; Obayashi, A.; Haraguchi, K.; Shibayama, M. Stress relaxation and hysteresis of nanocomposite gel investigated by SAXS and SANS measurement. *Polymer* **2012**, 53, 4533-4538.

(11) Li, P.; Siddaramaiah; Kim, N. H.; Yoo, G.-H.; Lee, J.-H. Poly(Acrylamide/Laponite) Nanocomposite Hydrogels: Swelling and Cationic Dye Adsorption Properties. *J. Appl. Polym. Sci.* **2009**, 111, 1786-1798.

(12) Haraguchi, K.; Uyama, K.; Tanimoto, H. Self-healing in Nanocomposite Hydrogels. *Macromol. Rapid Commun.* **2011**, 32, 1253-1258.

(13) Haraguchi, K.; Takada, T. Synthesis and Characteristics of Nanocomposite Gels Prepared by In Situ Photopolymerization in an Aqueous System. *Macromolecules* **2010**, 43, 4294-4299.

(14) Li, Z.; Shen, J.; Ma, H.; Lu, X.; Shi, M.; Li, N.; Ye, M. Preparation and characterization of sodium alginate/poly(N-isopropylacrylamide)/clay semi-IPN magnetic hydrogels. *Polym. Bull.* **2012**, 68, 1153-1169.

(15) Fossum, J. O. Physical phenomena in clays. *Physica A* **1999**, 270, 270-277.

(16) Cummins, H. Z. Liquid, glass, gel: The phases of colloidal Laponite. *J. Non-Cryst. Solids* **2007**, 353, 3891-3905.

(17) Nishida, T.; Endo, H.; Osaka, N.; Li, H.-j.; Haraguchi, K.; Shibayama, M. Deformation mechanism of nanocomposite gels studied by contrast variation small-angle neutron scattering. *Phys. Rev. E* **2009**, 80.

(18) Bakk, A.; Fossum, J. O.; da Silva, G. J.; Adland, H. M.; Mikkelsen, A.; Elgsaeter, A. Viscosity and transient electric birefringence study of clay colloidal aggregation. *Phys. Rev. E* **2002**, 65, 9.

(19) Meifang, Z.; Yang, L.; Bin, S.; Wei, Z.; Xiaoli, L.; Hao, Y.; Yu, Z.; Dirk, K.; Hans-Juergen, P. A. A Novel Highly Resilient Nanocomposite Hydrogel with Low Hysteresis and Ultrahigh Elongation. *Macromol. Rapid Commun.* **2006**, 27, 1023-1028.

(20) Zhang, Q. S.; Li, X. W.; Zhao, Y. P.; Chen, L. Preparation and performance of nanocomposite hydrogels based on different clay. *Appl. Clay Sci.* **2009**, 46, 346-350.

(21) Plivelic, T. S.; Labrador, A. L.; Theodor, K.; Gaponov, Y.; Svensson, C.; Nygaard, J.; Cerenius, Y. In *8th Nordic Workshop on Scattering from Soft Matter* Kjeller, Norway, 2011.

(22) Hammersley, A. P.; Svensson, S. O.; Hanfland, M.; Fitch, A. N.; Hausermann, D. Two-dimensional detector software: From real detector to idealised image or two-theta scan. *High Pressure Res.* **1996**, 14, 235-248.

(23) Graziano, G. On the temperature-induced coil to globule transition of poly-N-isopropylacrylamide in dilute aqueous solutions. *Int. J. Biol. Macromol.* **2000**, 27, 89-97.

(24) Pamies, R.; Zhu, K. Z.; Kjoniksen, A. L.; Knudsen, K. D.; Nystrom, B. Temperature-induced intermicellization and contraction in aqueous mixtures of sodium dodecyl sulfate and an amphiphilic diblock copolymer. *J. Colloid Interface Sci.* **2008**, 326, 76-88.

(25) Beheshti, N.; Zhu, K. Z.; Kjoniksen, A. L.; Knudsen, K. D.; Nystrom, B. Characterization of temperature-induced association in aqueous solutions of charged ABCBA-type pentablock tercopolymers. *Soft Matter* **2011**, 7, 1168-1175.

(26) Shibayama, M.; Suda, J.; Karino, T.; Okabe, S.; Takehisa, T.; Haraguchi, K. Structure and dynamics of poly(N-isopropylacrylamide)-clay nanocomposite gel. *Macromolecules* **2004**, 37, 9606-9612.

(27) Shang, C.; Rice, J. A. Invalidity of deriving interparticle distance in clay-water systems using the experimental structure factor maximum obtained by small-angle scattering. *J. Colloid Interface Sci.* **2005**, 283, 94-101.

(28) Ho, D. L.; Briber, R. M.; Glinka, C. J. Characterization of organically modified clays using scattering and microscopy techniques. *Chem. Mater.* **2001**, 13, 1923-1931.

(29) Lee, W. F.; Fu, Y. T. Effect of montmorillonite on the swelling behavior and drug-release behavior of nanocomposite hydrogels. *J. Appl. Polym. Sci.* **2003**, 89, 3652-3660.

(30) Crank, J. *The Mathematics of Diffusion*; second ed. ed.; Oxford University Press, USA, 1980.

(31) Haraguchi, K.; Li, H. J.; Okumura, N. Hydrogels with hydrophobic surfaces: Abnormally high contact angles for water on PNIPA nanocomposite hydrogels. *Macromolecules* **2007**, 40, 2299-2302.

TOC Graphic